Multi-spectral investigation of ozone: Part II. Line intensity measurements at one percent accuracy around 5 μm and 10 μm

David Jacquemart, Corinne Boursier, Hadj Elandaloussi, Pascal Jeseck, Yao Té, Christof Janssen

Multi-spectral investigation of ozone:

Part II. Line intensities measurements at one percent accuracy around 5 μm and 10 μm

David Jacquemart[a,*], Corinne Boursier[b], Hadj Elandaloussi[b], Pascal Jeseck[b], Yao Té[b], Christof Janssen[b]

[a] Sorbonne Université, CNRS, De la MOlécule aux NAno-objets : Réactivité, Interactions et Spectroscopies, MONARIS, 75005 Paris, France

[b] Sorbonne Université, Observatoire de Paris, Université PSL, CNRS, Laboratoire d'Etudes du Rayonnement et de la Matière en Astrophysique et Atmosphères, LERMA-IPSL, 75005 Paris, France

Number of Pages: 20

Number of Figures: 10

Number of Tables: 5

Supplementary materials (electronic files): 1

Keywords: ozone; 5 microns; 10 microns; line intensities; line positions; Fourier transform spectroscopy.

[*] Corresponding author: David Jacquemart (david.jacquemart@upmc.fr)

doi:10.1016/j.jqsrt.2021.108050

Abstract

Ozone line parameters have been retrieved from high-resolution Fourier transform spectra in the 5-μm and 10-μm spectral regions using a H-shaped cell with two parallel paths described in the first paper of the series (Multi-spectral investigation of ozone : Part I. Setup & uncertainty budget). The experimental arrangement allows for quasi simultaneous acquisition of spectra at 5 μm and 10μm with consistent ozone pressure. A multispectrum fitting procedure has been used to accurately measure line positions and intensities. Special care has been taken to determine the instrument line shape and its effect on line intensities and sources of uncertainties from the assumption of a molecular line profile have been investigated.

Line positions and intensities have been retrieved for 497 transitions at 10 μm, mostly (476) from the ν_3 band, but also from the ν_1 band (18 transitions) and from the $\nu_2+\nu_3-\nu_2$ hot band (3 transitions). At 5 μm, 319 transitions have been determined, of which 316 belong to the $\nu_1+\nu_3$ and 3 to the $2\nu_3$ bands. Comparisons with previous experiments and calculations as well as with databases are presented, showing systematic discrepancies. The new intensity data at the unprecedented 1% accuracy level unambiguously indicates that atmospheric databases currently suffer from systematic biases up to 4.2% in the $\nu_1+\nu_3$ band and 2.2% in the ν_3 band. The present results will help to resolve the long-standing UV-IR discrepancy observed in atmospheric and laboratory ozone studies. Comparisons with yet unpublished measurements and Hamiltonian-type calculations, as well as with recently published ab-initio calculations show an average discrepancy between 0.1% and 1.2% with sub-percent (0.4–0.8%) dispersion. The small scatter of the comparison confirms the sub-percent precision of both, the calculations, and the measurements.

1. Introduction

Ozone line intensities have been investigated at 5 μm and 10 μm based on high-resolution spectra recorded in both spectral regions from the same ozone sample, only very slowly evolving with time. In the past, the 10-μm spectral region of ozone has been studied more extensively than the 5-μm spectral region. Nevertheless, the necessity of reaching agreement on absolute intensities in the 10 μm region has been pointed out by several groups (see discussion in Paper I [1]) and is a serious concern for spectroscopic databases. The present analysis aims to reach accurate measurements of line intensities in both the 5-μm and the 10-μm region (with consistent data in the two spectral regions).

The experimental details of the acquisition of the high-resolution Fourier transform spectra and the associated measurement uncertainties are fully described in Paper I [1]. For convenience, we repeat some basic information here. Two sets of laboratory spectra at 6 different ozone pressures have been recorded with different scanning times at 5 μm and 10 μm. Line intensities of the $\nu_1+\nu_3$ band around 5 μm are around 10 times smaller than those belonging to the ν_3 band at 10 μm. A H-shaped cell with two parallel single absorption paths of lengths equal to 20.0357 cm for the 5 μm region and 5.0919 cm for the 10 μm region has been used. The signal-to-noise ratio (peak-to-peak) is around 150 and 500 for spectra recorded at 10 μm and 5 μm, respectively. As described in Paper I, ozone generated from oxygen at natural isotopic abundance has been used to fill the cell with pressures ranging from 20 Pa to 150 Pa (or 2×10^{-4} atm to 1.5×10^{-3} atm) of ozone (see Table 1 for experimental conditions). Since ozone partial pressures decreased slightly and linearly with time, average pressures of ozone and O_2 (see Paper I) during the recordings have been used to rigorously analyze the averaged FT spectra. Due to the low pressure of ozone used in this work, self-broadening coefficients of ozone have been fixed to values from HITRAN2016 [2]. Since small quantities of O_2 are present in the cell (see Table 1), the O_2 contribution to the collisional line widths of ozone has been taken into account by using air-broadening coefficients from HITRAN2016 [2]. The O_2 contribution is small, about 1% of the total collisional width. The multispectrum fitting procedure (MSF) described by Lyulin [3] was used to fit calculated spectra to experimental data in order to retrieve line positions and intensities of ozone transitions (even when using only a single spectrum during the fitting procedure).

(Table 1)

Average interferograms have been Fourier transformed using the OPUS/Bruker software with a “boxcar apodization” and a Mertz phase correction [4]. By choosing the boxcar function in OPUS, no artificial apodization is applied during the Fourier transform of the interferograms. The experimental spectra at 10 μm have also been corrected for thermal emission and detector non linearity as discussed in Paper I. The wavenumber calibration has been performed based on N_2O transitions as described in Paper I, leading to a standard uncertainty $u(\nu) = 3 \times 10^{-5}$ cm^{-1} for line positions.

In order to retrieve O_3 line intensities accurately, special care has been taken to consider sources of systematic biases that intervene in the fitting process, such as the apparatus function, the thermal emission, the non-linearity of the detector, and the line profile. As described in the first paper [1], the thermal emission and the non-linearity of the MCT detector have been corrected on spectra recorded at 10 μm. The absorption path lengths used in the present work take into account multiple reflection effects (see Paper I). After investigations of the apparatus function (or ILS for Instrument Line Shape) using the LINEFIT code [5], we deduced that applying a LINEFIT derived ILS was an improvement as compared to the use of a nominal (or ideal) ILS. Ozone transitions at 5 μm ($\nu_1+\nu_3$ band) and 10 μm (ν_3 band) have been used by LINEFIT to generate corresponding ILS functions. As a consequence, the analysis of the ozone transitions by multispectrum fitting procedure (MSF) is strongly correlated with the LINEFIT analysis since the molecular line parameters (and profiles) are used both by MSF and LINEFIT. Identical profiles (and collisional-broadening parameters) need to be employed in MSF and LINEFIT in order to obtain consistent results. This may be considered a disadvantage (using LINEFIT on ozone transitions that will be next measured by MSF), but under our experimental conditions, pressures of ozone are quite low (close to Doppler regime, especially at 5 μm) such that the effects of molecular collisions on the line profile are weak, and the use of fixed collisional parameters is well justified. Moreover, by analyzing spectral micro-windows (MWs, hereafter) containing ozone transitions, LINEFIT allows to directly estimate deviations from line positions and intensities used as input or reference data. Indeed, in order to determine the ILS, LINEFIT is using scaling factors to correct eventual systematic deviations from input line positions and intensities of transitions belonging to the selected MW. Those scaling factors yield a global estimation on how line positions and intensities in the considered experimental spectrum deviate from those used by LINEFIT as a reference, which corresponds to parameters provided by HITRAN 2016 in our case. Note that the use of LINEFIT does not allow to directly determine line parameters from an experimental spectrum. However if line positions and intensities from input databases present a systematic erroneous shift within the analyzed MWs, LINEFIT gives an accurate estimation of the systematic deviations between the line intensities in an experimental spectrum and the input line parameters. In the case of ozone spectroscopic data in HITRAN 2016, line intensities at 5 μm and 10 μm come from Hamiltonian calculations based on multiple consistent sets of measurements for which an interrogation remains on absolute ozone concentrations. As it will be confirmed in this study, the intensities in HITRAN 2016 are consistent within each of both spectral regions considered here, but they deviate from our measurements to a different degree. These deviations are already indicated by the LINEFIT analysis.

As a result of the analysis of the experimental set of spectra described in Paper I, 497 and 319 transitions of the ozone main isotopologue have been studied by MSF between 997.5 cm^{-1} and 1134.4 cm^{-1} and between 2067.6 cm^{-1} and 2132.3 cm^{-1}, respectively. Among the transitions studied around 10 μm, 476 belong to the ν_3 band, 18 to the ν_1 band and 3 to the $\nu_2 + \nu_3 - \nu_2$ band. At 5 μm, 316 transitions belong to the ν_1

+ ν_3 band and 3 to the $2\nu_3$ band. Line intensities given in this work are reported in cm/molecule at 296K for ozone at natural isotopic composition with a relative abundance of the main $^{16}O_3$ isotopologue of 99.29 % (see Paper I), as defined by HITRAN. The complete set of final measurements is available as Supplementary Material. All analyses performed in Section 2 are based on the same set of transitions than those presented in Supplementary Material.

The manuscript is structured as follows. Section 2 corresponds to the analysis of experimental spectra at 5 μm and 10 μm (see Table 1) using LINEFIT to deduce the ILS, and then using MSF to retrieve line positions and intensities. Various tests have been performed and summarized in this section, such as the impact on line intensities measurements (under our experimental conditions) of line profiles (Voigt versus qSDVP) or erroneous broadening coefficients of ozone. Section 3 presents the comparisons between our set of measurements at 5 μm and 10 μm and data from the literature (including measurements and independent calculations). It also describes comparisons with line positions and intensities present in HITRAN1996 [6] and 2016 [2], GEISA2015 [7] and S&MPO [8] databases. A short summary and some conclusions are given in Section 4.

2. Analysis of experimental spectra by LINEFIT/MSF

In both LINEFIT and MSF codes, the experimental spectrum is considered as a convolution of a theoretical line profile (Voigt for example) and an instrument line shape. At a certain degree of accuracy (and depending on experimental conditions and on how the interferometer is aligned), the ideal ILS is not sufficient to describe the experimental spectrum accurately. In our case (see Paper I for more details), the unapodized FWHM (full width at half maximum) of the instrument function is approximately given by $0.603/\Delta_{max} = 2.3\times10^{-3}$ cm^{-1}, where Δ_{max} is the maximum path difference of the Fourier Transform (FT) spectrometer (Δ_{max} = 257.143 cm). For comparison, the ozone collisional FWHM by collisions with O_3 (around 0.04×10^{-3} cm^{-1} to 0.3×10^{-3} cm^{-1}) and O_2 (around 0.006×10^{-3} cm^{-1}) are smaller than the Doppler FWHM of ozone at 10 μm (1.8×10^{-3} cm^{-1}) and 5 μm (3.6×10^{-3} cm^{-1}). Thus, the line profile FWHM is almost twice the FWHM of the ILS at 5 μm, whereas at 10 μm the two FWHM are almost equal. Identical optical settings have been used during the recordings of the two sets of experimental spectra (see Table 1) so that we assume that the ILS should be the same for all experimental spectra recorded around 10 and 5 μm. As discussed in Section 1, the broadening coefficients have been fixed in our studies to those of the HITRAN 2016 database.

To a first approximation, the ILS is the Fourier transform of the boxcar function $\Pi_{0\to\Delta_{\max}}$ due to the finite optical path difference of the interferometer. This corresponds to the sinc function which is not wavenumber dependent. To the next order of approximation the finite beam size has to be taken into account. An optical weighting function $P_{opt}(\Delta)$ of the boxcar function allows modeling the effect of the beam size. It is given by [9]:

$$P_{opt}(\Delta) = \left|\frac{\sin x}{x}\right| ; x = \frac{\nu\Omega\Delta}{2} ; \Omega = \pi\frac{R^2}{f^2} \quad (1)$$

where ν is the wavenumber, Δ is the optical path difference, R the radius of the beam, and f the focal length of the input interferometer collimator. The optical weighting is wavenumber dependent and increases with wavenumber, leading to a stronger apodization of the calculated instrument line shape $ILS(\nu)$, also called ideal or nominal ILS (when the interferometer is perfectly aligned with no diffraction effects for example).

$$ILS(\nu) = \mathrm{FT}\left[\Pi_{0\to\Delta_{\max}} \times P_{opt}(\Delta)\right] \quad (2)$$

In a first step, the ideal ILS has been calculated (Eqs. (1) and (2)) for various spectral ranges under study at 5 μm and 10 μm, taking into account the wavenumber dependency of the calculated ILS. An example of residuals obtained using a Voigt molecular line profile is given in Fig. 1 for 10 μm and 5 μm by single spectrum (panels (*b*)) or multispectrum (panels (*d*)) fitting procedures. Using the single spectrum procedure allowed us to free ourselves from eventual pressure inconsistencies. Indeed, in the single spectrum fitting procedure, each spectrum is fitted individually and

independently from the others, whereas in the multispectrum fitting procedure correlations due to common line parameters in the different spectra are taken into account. As observed in Fig. 1 (panels (*b*) and (*d*)), the residuals using single spectrum fitting (panels (*b*)) are almost identical showing a good consistency between experimental conditions of all fitted spectra (see Table 1). At 10 μm, no characteristic signature emerges from the signal noise (S/N around 0.7% peak-to-peak) whereas at 5μm the use of the nominal ILS leads to systematic signatures that clearly stand out from the experimental noise (S/N around 0.2% peak-to-peak). Reducing the aperture radius *R* down to 0.545 mm for ILS calculation (Eqs. (1) and (2)) slightly improves the fit residuals at 5 μm, but W-shaped signatures are still observed. Such signatures may be due to either (or both) an inaccurate line profile or an incorrect instrument line shape. Note that even by assuming a positive or negative phase error (as defined in Ref. [10] and generally due to an error in the zero optical path difference or to an irregularity in the displacement of the mobile mirror), the signatures at 5 μm (see Fig. 1, panels (b) and (d)) do not decrease significantly. We note that using even more complex molecular line profile (qSDVP) in combination with the ideal ILS can improve the residuals but leads to unrealistically large quadratic speed dependence parameters, indicating that the effect is rather linked to non-ideal ILS of the spectrometer.

(Fig. 1)

A more realistic ILS is provided through the LINEFIT program [5].The code (version 14.8) has been used to infer the ILS from each experimental spectrum (employing the extended ILS model), by performing a constrained fit of parameters which describe the interferometer's modulation efficiency in the interferogram domain [5,11]. This complex modulation efficiency is defined as the ratio of the normalized modulation of the actual Fourier transform spectrometer (FTS) and the normalized modulation of a nominal FTS as a function of the optical path difference. Several micro windows of around 5 cm^{-1} spectral width (see Table 2) have been used simultaneously to retrieve the ILS of each spectrum through LINEFIT (using the experimental conditions listed in Table 1). By using line parameters from databases, LINEFIT allows to deduce the ILS for an experimental spectrum. Changing line parameters or the profile function in LINEFIT correspondingly affects the retrieved ILS. For each MW, column parameters (scaling factors for intensities) account for eventual systematic deviations between the measurement and database values As discussed in Section 1, HITRAN 2016 ozone data (positions, intensities, and widths) have been used as input parameters together with assuming a Voigt molecular line profile. Table 2 summarizes the column parameters used by LINEFIT for the various MWs (5 MWs for 10 μm and 4 MWs for 5 μm) used to retrieve the ILS (lines noted ILS-Sp*i* in Table 2). Figure 2 presents the deviation of the LINEFIT-ILSs from the ideal function in terms of modulation efficiency loss and phase: in the case of an ideal ILS, modulation and phase parameters should be equal to 1 and 0, respectively for all optical path difference (hereafter noted OPD) values. Note that the phase parameter retrieved via LINEFIT (depending on

OPD) is different from the phase error as defined in Ref. [10] and should not be confused.

(Table 2)

(Fig. 2)

Globally, at 10 μm the LINEFIT-ILS is closer to the ideal ILS than at 5 μm where the modulation efficiency loss differs from 1 after OPD = 100 cm and where the phase is either positive or negative according to the OPD value. If considering that the ILS should be the same for the 6 spectra recorded in the same spectral region (5 μm or 10 μm), the modulation and phase parameters obtained by LINEFIT should be more or less similar. A good consistency between experimental spectra is observed for modulation efficiency losses at 10 μm, whereas at 5μm the modulation efficiency losses seem to be more dependent on ozone pressure (the highest modulation efficiency losses are obtained for spectra 1 and 6 recorded at the highest ozone pressures, see Fig. 2). Note that for the spectra recorded at the lowest ozone pressures (spectrum 4, see Table 1) at 5 μm and 10 μm, the modulation efficiency losses are shifted from 1 from the first OPD values (except for OPD = 0 cm for which the modulation is fixed to 1). As it will be discussed later, the ILS obtained from the lowest pressure spectrum leads to the highest deviation for intensities retrieval (both through LINEFIT and MSF). Therefore and because the unphysical offset at low OPD, we conclude that the ILS for spectrum 4 (both at 5 μm and 10 μm) should be disregarded as the least precise. The phase parameters show a good consistency between the 6 spectra at 5 μm, contrary to the 10 μm region where the phase is strongly dependent on the experimental spectrum (but also on the choice of the MWs in LINEFIT), with no obvious link to pressure of ozone in the cell (see phase parameter for spectra 1 and 6 in Fig. 2). In order to retrieve the ILS, column parameters are used by LINEFIT to scale (in each MW) line intensities from HITRAN 2016 (same scaling factor for all transitions belonging to the same MW). As observed in Table 2 the column parameters from LINEFIT-ILS retrievals (noted ILS-SP*i* in Table 2) are consistent within 0.5% depending on the MW (except for spectrum 4), suggesting that ozone line intensities from HITRAN 2016 [2] are lower by about 2 to 2.5 % at 10 μm and by ca. 4 to 4.5 % at 5 μm. The column parameters obtained for spectrum 4 for which the modulation efficiency loss at 5 μm and 10 μm is shifted from 1 (see Fig. 2) are systematically lower than those obtained for other spectra (especially at 5 μm where the absorbance is smaller than at 10 μm). Note that choosing different MWs for the analysis does not significantly modify (maximum 0.2%) the column parameters issued by LINEFIT. The variability of the LINEFIT-ILS parameters (modulation and phase) according the chosen set of fitted MWs is within the variability of the ILS retrieval for the various spectra of the series and is taken into account in the ILS repeatability discussed in Section 3.8.2 of Paper I.

In order to test the impact of the ILS on the line intensity measurements obtained from multispectrum fitting all spectra, the spectra have also been successively analyzed by MSF using the ILS obtained from spectrum 1 to 6. Since the ILS should not depend

on the ozone pressure in the cell, we have used the same ILS for the multispectrum analysis of the 6 recorded spectra. The retrieved line intensities have been systematically compared (see Fig. 3) to our final set of measurements (hereafter noted $S_{\text{this work}}$). The latter has been obtained by MSF using the averaged LINEFIT-ILS retrieved from spectra 1, 2, 5, and 6 (which correspond to the highest ozone pressures and the strongest "signals"). To estimate the variability of the column parameters (see **ILS-avg** in Table 2), the modulation and phase parameters have been fixed to the average values corresponding to the averaged LINEFIT-ILS. The obtained column parameters show a slightly better consistency between spectra when using this ILS. The average of column parameters obtained for all MWs in all spectra is equal to 1.0206(34) and 1.0222(31) at 10 μm (1.0392(64) and 1.0419(18) at 5 μm) respectively for ILS retrievals (ILS-SPi in Table 2) and when fixing ILS to the averaged LINEFFIT-ILS (ILS-Avg in Table 2). We believe that using the averaged LINEFFIT-ILS reduces the noise in LINEFIT retrievals, and provides the most realistic LINEFIT-ILS for all spectra and a better estimation of the systematic bias of the HITRAN2016 line intensities (overestimated by 2.2(3)% and 4.2(2)% at 10 μm and 5 μm respectively) through LINEFIT column parameters. Table 3 summarizes the averaged intensity ratios obtained for each single spectrum ILS. In the 10 μm spectral region, a very good consistency (within -0.1% and +0.16 % on average) is found between line intensities retrieved using the LINEFIT ILS from spectrum 1, 2, 5 or 6 (and the averaged LINEFIT-ILS), as well as when using the ideal $\text{ILS}_{R\,=\,0.575\ \text{mm}}$. The corresponding intensity ratios do not depend on the observed absorbance of the transitions (just slightly when using the ideal ILSs). Using LINEFIT-ILS from spectrum 3 or 4 as well as the ideal $\text{ILS}_{R\,=\,0.545\ \text{mm}}$ leads to somewhat larger deviations with intensities being 0.5 to 2% smaller than our best estimate $S_{\text{this work}}$ (see upper panel of Fig. 3). At 5 μm, we also observe a good consistency (within -0.1% and +0.26 % for ratio averages, see lower panel of Fig. 3) between line intensities retrieved using the LINEFIT-ILS from spectrum 1, 2, 3, 5 or 6 (or the averaged LINEFIT-ILS), as well as when using the ideal $\text{ILS}_{R\,=\,0.545\ \text{mm}}$. Only the LINEFIT ILS from spectrum 4 and the ideal ILS with R = 0.575 mm lead to significantly different intensities in this region. The signatures in the fit residuals at 5 μm obtained with an ideal ILS (see panels (*b*) and (*d*) in Fig. 1) completely disappear within the experimental noise (see panels (*a*) and (*c*) in Fig. 1) when using the LINEFIT-ILS, regardless the choice of the spectrum for deriving the ILS. At 10 μm, the residuals are slightly improved when using the LINEFIT-ILS (see panels (*a*) and (*c*) in Fig. 1) instead of the ideal ILS functions. For the averaged LINEFIT-ILS, we estimate the noise effect from LINEFIT-ILS retrievals on the intensity measurements to be about 0.1 % in the final uncertainty budget [1].

(Fig. 3)

It is interesting to compare residuals and intensity measurements from the single spectrum fitting to those obtained by multispectrum fitting. Indeed, this comparison allows to observe eventual inconsistencies between the different experimental spectra. The slight improvement of residuals in panel (a) of Fig. 1 obtained by single spectrum

fitting as compared to panel (c) obtained by multispectrum fitting is probably due to slight inconsistencies between the experimental pressures and/or temperatures (the same optical settings and absorption path lengths have always been used for a series of spectra). As for line intensity retrievals, we systematically compare the line intensities obtained in the single spectrum fitting procedure to the line intensity values finally retained in this work ($S_{\text{this work}}$, see Fig. 4). Note that the average LINEFIT-ILS (from spectra 1, 2, 5 and 6) has been used as a reference to compare all fits presented in Fig. 4. The average ratios are consistent within ±0.2 %, again demonstrating the good consistency between the 6 individual spectra. Fig. 4 further indicates that the dispersion is systematically higher at 10 μm than at 5 μm, which is due to the experimental noise being sensibly higher at 10 μm (0.7%) than at 5 μm (0.2%). Moreover, the dispersions of the intensity ratios in Fig. 4 are higher than those presented in Fig. 3. This is due to the fact that Fig. 3 displays the results of multispectrum fits, whereas Fig. 4 shows the results of fitting individual spectra. Figure 4 also reveals that the dispersion increases with decreasing ozone pressure and intensities. This correlates with becoming less sensitive in the measurement of weaker absorptions and smaller intensities.

(Fig. 4)

In order to estimate the effect of eventually erroneous ozone self-broadening coefficients reported in HITRAN 2016 [2], we have applied the previous analysis (using LINEFIT on spectra 1, 2, 5 and 6 with Voigt profile in order to derive a corresponding ILS) with self-broadening coefficients being increased or decreased by 5 %. Then, using this average LINEFIT-ILS, the multispectrum fitting procedure has been applied to spectra 1-6 with the same increased/decreased self-broadening coefficients to retrieve line intensities at 5 μm and 10 μm. A similar procedure has been performed when using qSDVP [12] instead of the Voigt profile in LINEFIT and MSF in order to estimate the impact of the line profile model on the line intensity determination. For this study, the quadratic-speed-dependence of the self-pressure-induced half-width γ_2 has been assumed to be proportional to the ozone self-broadening coefficients (γ_0) from HITRAN 2016. According to investigations of the qSDVP for rovibrational CO_2 transitions at 1.43 μm [13] and at 3 μm [14], the quadratic-speed-dependence of the self-pressure-induced half-width γ_2 tends to vary between 10% to 15% of the self-broadening coefficients with no significant dependence on the vibrational quantum numbers. Since no ozone study using the qSDVP has been published, we have fixed the γ_2 parameters both in LINEFIT and MSF to successively 10 % and 15 % of the HITRAN 2016 self-broadening coefficients. The quadratic term δ_2 linked to the self-shift has been neglected, as in Refs. [13-14]. The sensitivity of line intensities to either “erroneous” self-broadening coefficients with the Voigt profile or the qSDVP instead of the Voigt profile can be visualized in Figs. 5 and 6, respectively. The line intensity ratios in Figs. 5 and 6 have been plotted versus the center of line Voigt-absorbance of the studied transitions at the pressure of spectrum 1 (see Table 1). Since the relative contribution of the collisional part is more important at 10 μm than at 5 μm due to the Doppler width at 5 μm being twice the Doppler width at 10 μm, comparisons between deviations

obtained at 5 μm and at 10 μm may include some bias. We can nevertheless assume that the broadening effects (erroneous broadening parameters or line profile) have a stronger impact on the line intensity retrieval at 10 μm than at 5 μm. The absorbance-dependencies of the observed ratios look similar at 5 μm and at 10 μm, both in Figs. 5 and 6, but the smaller range of absorbances measured at 5 µm does not allow to confirm that both dependencies are actually equal. A systematic deviation of less than 0.25% is observed when comparing ratios at 5 μm with ratios at 10 μm in Fig. 5. The deviation is 0.5% when comparing the qSDVP with the Voigt profile at 5 μm and at 10 μm (Fig. 6). At 5 μm, the sensitivity of the line intensity is quite weak as compared to 10 μm, both when introducing "erroneous" self-broadening coefficients (see Fig. 5) or when using the qSDVP (see Fig. 6). The residuals obtained for all fits (including those with "erroneous" self-widths) are not significantly modified as compared to those obtained in panels (*c*) of Fig. 1. Indeed, when using "erroneous" self-widths, LINEFIT corrects the ILS and since MSF is using this corrected ILS with the same "erroneous" self-widths, the final line profile (convolution of line profile and ILS) is not affected much, leading to very similar residuals. When using the qSDVP instead of the Voigt profile, there is no improvement in the fit residuals, probably due to similar theoretical line profiles under our experimental conditions. Nevertheless, observing similar residuals does not imply that line intensities are not modified. This is shown in Figs. 5 and 6, especially at 10 µm. There, under our experimental conditions, deviations range from -0.7% to +0.5% when "erroneous" self-broadening coefficients are introduced and from -0.5% to +0.1% when the qSDVP is used instead of the Voigt profile. Note that the comparison presented in Fig. 6 probably suffers from the fact that self-broadening coefficients depend on the molecular line profile. As shown in Ref. [14] for CO_2 transitions, the retrieved self-broadening coefficients were systematically lower with the Voigt profile than with qSDVP. For the comparisons presented in Fig.6, the same broadening parameters have been used for the two profiles.

(Fig. 5)

(Fig. 6)

3. Comparisons

Quite a number of ozone line intensity studies have been published, especially on the fundamental region at 10 μm. Here, we have chosen to compare with the more recent work published since 2000. It should also be emphasized that the experimental setup [1] of the present study allows recording both spectral regions using the same ozone sample. This reduces possible systematic biases between line intensity measurements performed at 5 μm and at 10 μm, notably those related to the determination of the ozone pressure. Below is a shirt description of the various studies used for the comparison. Most of these experimental studies have employed UV absorption at 254 nm to determine the ozone partial pressure. If not mentioned otherwise, these studies have utilized the absolute cross section of 1.136 10^{-17} cm^2 at 297K from the Mauersberger group at Minnesota [15-16]. This value is only 0.27 %

higher than the most recent recommendation of Hodges et al. [17], on which our study depends on.

- Claveau et al. [18] measured 295 line intensities at 10 μm with an accuracy between 2 and 5 % using a FT spectrometer. The partial pressure of ozone in the setup has been derived from measurements with a high precision (0.5 %) capacitive pressure transducer.
- De Backer-Barilly and Barbe [19] determined 290 line intensities at 10 μm with accuracy better than 2 % using a FT spectrometer. The ozone partial pressure has been determined using both, a capacitive pressure gauge and UV absorption at 254 nm.
- Smith et al. [20] have used UV absorption at 254 nm to infer the ozone concentration for their quantitative intensity study of 376 transitions around 10 μm using a FT spectrometer. The accuracy for the strongest transitions is around 2 %, and 4 to 5% for the weakest.
- Thomas et al. [21] measured both at 5 μm and 10 μm using a UV-IR crossed beam alignment and a FT spectrometer. Contrary to the present work, the 5 μm and 10 μm regions have been recorded in independent runs using separate ozone samples for each of the two spectral regions. Altogether, 65 transitions at 10 μm and 18 transitions at 5 μm have been determined with a reported average accuracy of 1.5%.
- Very recently, several data sets for the 10-μm region have become available within the frame of the ESA SEOM-IAS (Improved Atmospheric Spectroscopy Databases) project [22,23]. So far, the data have not yet been published in the peer reviewed literature. One set is based on measurements at DLR (Deutsches Zentrum für Luft und Raumfahrt, the data set is hereafter noted DLR_ESA), and the two others are based on effective Hamiltonian calculations; one from J.-M. Flaud (noted JMF_ESA hereafter) and one from A. Barbe and V. Tyuterev (noted URCA_ESA hereafter). The set of new measurements from DLR_ESA and the two sets of calculations (JMF_ESA and URCA_ESA) have also been compared to the present measurements. Note that in version2 of the ESA SEOM-IAS project [23], the DLR data set corresponds to a line list from a calculation using an effective Hamiltonian (JMF_ESA) whereas in version 1 [22], the DLR data set corresponds to a line list from a direct fit to the measurements (DLR_ESA).
- New measurements of 571 unpublished line positions and intensities at URCA (Université de Reims Champagne-Ardenne) have been communicated privately [24] by A. Barbe and M.-R. De Backer
- Two recent ab-initio studies [25,26] have published sub-sets of calculated line intensities both in the 10 μm and the 5 μm regions. After contacting the authors of these studies, extended data sets have been communicated allowing to do a more complete comparison between these calculations and the present measurements. Results based on the various PESs (Potential

Energy Surface) and DMSs (Dipole Moment Surface) have been presented in Ref. [26]. It is interesting to observe in Tables 2 and 3 from Ref. [26] that changing either the DMS or the PES can lead to systematic changes of line intensities by 4% to 5% and 1%, respectively.

The line positions and intensities of this work have also been compared to data from several spectroscopic databases. With respect to the yet unexplained discrepancy between measurements, it is interesting to compare the present measurements to both HITRAN 1996 [6] and 2016 [2] editions that contain different parameters. The line intensity data at 5 μm and 10 μm in the GEISA 2015 database [7] have been provided by Wagner et al. [27]. These values remain unchanged since the 2003 edition. Line positions and intensities in the S&MPO database (Spectroscopic & Molecular Properties of Ozone) [8] have been updated very recently in February 2021. Concerning the lines measured in the present work, the main change from S&MPO 2019 (pre February 2021) and S&MPO 2020-d (past February 2021) is due to ab-initio intensity corrections [28] following a comparison between preliminary measurements from this work and ab-initio calculations [25]. Both versions of S&MPO (2019 and 2020-d) have used in the comparison.

The following Section 3.1 is dedicated to comparisons between the present measurements and measurements from the literature, whereas comparisons between measurements and various sets of calculations (including spectroscopic databases) are presented in the subsequent Section 3.2.

3.1. Comparison with measurements

Line position differences and line intensity ratios between the measurements from [18-22,24] and our study are plotted in Figs. 7 and 8, respectively. Note that an obvious outlier has been identified in the DLR_ESA measurements [22], namely the ν_3 transition located at 1059.182 cm^{-1} that has a measured intensity of 8.330×10^{-21} cm/molecule. In HITRAN2016 and in the present work, the transition is reported with a 15% higher intensity of 9.856×10^{-21} and of 1.010×10^{-20} cm/molecule, respectively. Since this deviation largely exceeds stated accuracies, this particular transition has been removed for the comparison with the DLR measurements [22].

In addition to the graphical comparison, we also compare our data to each data set using the average difference of line positions, the average ratio of line intensities, the number of compared transitions, and the intensity ranges in Table 4. Measurements concerning different bands within the same spectral region have been analyzed separately for each publication. Consequently, there should be no systematic deviation between our study and the literature data due to inadvertently merging different bands belonging to the same spectral region. This is supported by Figs. 7 and 8, where comparisons are consistent within different bands belonging to the same spectral region. Averages in Table 4 were calculated without differentiating between bands, however.

(Fig. 7)

(Fig. 8)

(Table 4)

The comparison of line positions in Fig. 7 shows that our measurements agree very well with previous experiments. Average discrepancies between the measured positions in this work and the measurements of previous studies [18-22,24] are just a few 10^{-5} cm^{-1} (see Table 4). The observed standard deviations (SD) are typically a few 10^{-5} cm^{-1}, except when comparing to the work of Claveau et al. [18], where the dispersion is about one order of magnitude larger (3×10^{-4} cm^{-1}). The global agreement in line positions can also be observed in Fig. 7. Note that the transition measured at 1054.05860 cm^{-1} in the present work is in good agreement with Thomas et al. [21] who report the line to be at 1054.05852 cm^{-1}. However, De Backer-Barilly et al. [19] give its position at 1054.05810 cm^{-1}, indicating that this transition likely represents an outlier by about 4×10^{-4} cm^{-1} in that data set. Noteworthy, the agreement with the line positions from Refs. [20,22] (273 [20] and 492 [22] lines, respectively, which are common with the present data) is excellent: average discrepancies are around 2 to 3×10^{-5} cm^{-1} and the dispersions (1SD) are of similar magnitude (see Table 4), which corresponds very well to our standard uncertainty of $u(\nu) = 3\times10^{-5}$ cm^{-1}.

The comparison of line intensities is shown in Fig. 8 and the average intensity ratios are summarized in Table 4. The set of measurements from Refs. [18,19,21] is quite consistent, but lower than the present intensities by 2.7-3.7 % on average (see Fig. 8). The work of Smith et al. [20] shows line intensities that are globally higher (2.2% on average) than the present measurements. The yet unpublished measurements performed at DLR [22] and by Barbe and De Backer [24] respectively agree with the present measurements to within 0.1% and 0.3% on average. This is also evident from Fig. 8. At 10 μm, the dispersion (1SD) of line intensity ratios varies between 1.4 % and 1.9 %, except for the comparison between this work and the measurements from Ref. [24]. There, the standard deviation of the intensity ratio is just 0.9%. At 5 μm, only the 10 common transitions with Ref. [21] could be compared. On average, line intensities from Ref. [21] at 10 μm and 5 μm are 3.7% to 3.8% lower than the present measurements. This is quite significant, given the relative uncertainties of 1.4 % and < 1%, respectively, which are consistent with the rather low dispersion of only 0.6 % (1SD) (see Table 4).

3.2. Comparison with calculations

Systematic comparisons between the present measurements and effective Hamiltonian-type calculations have been performed and plotted in Figs. 9 and 10, where line positions and line intensities are displayed, respectively. For ab-initio calculations [23-24] only line intensities have been compared and these are also presented in Fig. 10.

All averages of the comparisons between the present measurements and calculations/databases at 5 μm and 10 μm are summarized in Table 5. We omit here the comparison with ab-initio calculated line positions because these are usually much less accurate than high-resolution spectroscopic measurements.

(Fig. 9)

(Fig. 10)

(Table 5)

Figure 9 shows that there is generally very good agreement in line positions (within a few 10^{-4} cm^{-1}) between our measurements and the Hamiltonian type calculations, except for a few individual lines belonging to the $\nu_1+\nu_3$ band which are affected by strong resonances. These individual discrepancies can be quite strong (see Fig. 9) when comparing present measurements and calculations. For example, there are two transitions measured at 2090.7188 cm^{-1} and 2124.2628 cm^{-1} in this work, but have calculated positions at 2090.7197 cm^{-1} and 2124.2637 cm^{-1} in HITRAN2016 [2] and S&MPO [8] (both 2019 and 2020-d), and at 2090.7248 cm^{-1} and 2124.2688 cm^{-1} in GEISA2015 [7] (see Fig. 9). Except for these few lines of the $\nu_1 + \nu_3$ band, the various calculations are reproducing the present measurements within a few 10^{-4} cm^{-1}. The standard deviation (1SD) of the average comparisons is around or less than 10^{-4} cm^{-1} for all bands (see Table 5), except for the $\nu_1+\nu_3$ band in the GEISA2015 database (because of the very large deviations of the two lines discussed above). If these two transitions are removed from the comparison, the average difference between measured line positions of this work and line positions of GEISA2015 [7] does not change but the standard deviation (1SD) decreases by a factor of 3: from 48×10^{-5} cm^{-1} to 14×10^{-5} cm^{-1}.

The line intensity comparisons presented in Figs. 8 and 10 (see also Tables 4 and 5) show one clear trend in the 10 μm region: the present measurements are in very good agreement with the very recent measurements from Refs. [22,24] and associated calculations from ESA SEOM-IAS [23], thus confirming a systematic bias of the ν_3 band in the HITRAN2016, GEISA2015 and S&MPO2019 databases of about 2.2%. In the 5 μm spectral region, there are no recent measurements to compare. Nevertheless, we observe a systematic bias in both the HITRAN2016 or S&MPO2019 databases of 4.2% for the $\nu_1+\nu_3$ band. In GEISA2015, the bias is smaller (1.9%). The recent version of S&MPO (2020-d) which is based on investigations towards the intensity consistency of the ozone bands in the infrared range [28] is in excellent agreement with present measurements both at 5 μm and at 10 μm.

Comparisons with ab-initio calculated intensities are plotted in Fig. 10 and comparisons of averages are given in Table 5. The two closest calculations to present measurements are those using the DMS from Tyuterev et al. [25,29] whereas the use of the DMS from Ref. [26] leads to a larger deviation from the present measurements (see Table 5 and Fig. 10). By using the same DMS from Ref. [25,29] but different PESs [25,26], the present measurements at 10 μm (ν_3 band) are systematically lower than the

ab-initio calculations by 1.1% to 1.2% (see Table 5). At 5μm, our measurements ($\nu_1+\nu_3$ band) match the results of Ref. [25] within 0.5% on average, whereas the discrepancy is higher (average is equal to 1.1%) when comparing calculations presented in Ref. [26] using the PES from Ref. [26] and the DMS from Ref. [29]. The quality of ab-initio intensities may be highly degraded for transitions that are affected by resonances with nearby levels. Such transitions have therefore been removed from the comparisons. Note that a recent effort [30] allowed to identify and correct such transitions from ab-initio calculations.

As a final remark, we point out that the dispersion parameters in the comparison between our measurements and the ab-initio and Hamiltonians calculations indicate that the precision of our measurements (and of the calculations) is well below 1%. The comparison with the ab-initio calculations that are completely independent from our measurements yields standard deviations between 0.005 and 0.006 for the 184 or 476 common transitions in the ν_3 band and is equal to 0.004 for 179 or 316 transitions in the $\nu_1+\nu_3$ band for the two respective calculations [25,26]. This is in full agreement with the uncertainty budget given in Paper I, where a line by line dispersion between 0.3 % and 0.5 % in the 5 μm range and between 0.5 % and 0.6 % in the10 μm region has been derived. The agreement of the averages at the 1% level, however, might yet be fortuitous, because ab-initio calculations still require educated guesses concerning global parameters [25], the choice of the DMS or PES in Ref. [26] just being one example.

Note that preliminary results of the current measurements were used in Refs. [25,30] in order to be compare with ab-initio calculations or databases. The first preliminary measurements used by Ref. [25] are on average higher by 0.5% at 10 μm and lower by 0.5% at 5 μm than the results presented here. The second set of preliminary measurements used by Ref. [30] is globally higher than the final results (this work): 0.9% at 10 μm and 0.5% at 5 μm. These different set of measurements are due to the evolution of the spectral analysis and inclusion of corrections for systematic effects that occurred just until the final revision of the manuscript.

4. Conclusion

Measured line positions and intensities have been retrieved with an accuracy of 3×10^{-5} cm^{-1} and $\lesssim$ 1%, respectively. The excellent accuracy reached for line intensity measurements is the fruit of several efforts to minimize systematic effects as non-linearity of detection, thermal emission, instrument line shape and line profile. In addition to the excellent accuracy, the design of the experimental setup (H-type cell and simultaneous recordings at 5 μm and 10 μm) has allowed to establish a high degree of consistency between intensities retrieved at 5 μm and at 10 μm. Significant deviations from databases were observed at 5 µm (4.2%) and at 10 μm (2.2%). A very good agreement (1% or less in average) is obtained with recent ab-initio calculations or yet unpublished effective Hamiltonian type calculations. The present set of accurate measurements and the consistent comparisons with recent measurements and calculations demonstrate once more the need to update the current ozone data in the data bases. The identification of a 2.2% systematic bias in the strongest fundamental (ν_3) in the atmospheric databases contributes to solving the long standing problem of a 4 to 5% discrepancy between remote sensing of ozone in mid-IR and the UV.

Acknowledgments:

This work was supported by the French national program LEFE/INSU. The authors are grateful to Vladimir Tyuterev and Oleg Polyansky for sharing a larger set of ab-initio calculations than the ones published, as well as to Jean-Marie Flaud, Alain Barbe and Marie-Renée De Backer who shared unpublished calculations or measurements at 10 μm. We also would like to thank Ha Tran for helpful discussions concerning qSDVP, and Oleg Lyulin for sharing his last version of multispectrum fitting code MSF. The authors also acknowledge two anonymous reviewers for their insightful and critical remarks.

References:

[1] Janssen C, Boursier C, Elandaloussi H, Jeseck P, Koshelev D, Marie-Jeanne P, et al. Multi-spectral investigation of ozone: Part I. Setup & uncertainty budget. J Quant Spectrosc Radiat Transf 2021: submitted for HITRAN special issue.

[2] Gordon IE, Rothman LS, Hill C, Kochanov RV, Tan Y, Bernath PF, et al. The HITRAN2016 Molecular Spectroscopic Database. J Quant Spectrosc Radiat Transf 2017;203:3–69.

[3]. Lyulin OM. Determination of Spectral Line Parameters from Several Absorption Spectra with the MultiSpectrum Fitting Computer Code. Atmos Ocean Opt 2015;28:387–395.

[4] Mertz L. Transformations in Optics. John Wiley and Sons, New York, 1965.

[5] Hase F, Blumenstock T, Paton-Walsh C. Analysis of the instrumental line shape of high-resolution Fourier transform IR spectrometers with gas cell measurements and new retrieval software. Appl Opt 1999;38:3417–22.

[6] Rothman LS, Rinsland CP, Goldman A, Massie ST, Edwards DP, Flaud JM, et al.. THE HITRAN MOLECULAR SPECTROSCOPIC DATABASE AND HAWKS (HITRAN ATMOSPHERIC WORKSTATION): 1996 EDITION. J Quant Spectrosc Radiat Transf 1998;60:665–710.

[7] Jacquinet-Husson N, Armante R, Scott NA, Chédin A, Crépeau L, Boutammine C, et al. The 2015 edition of the GEISA spectroscopic database. J Mol Spectrosc 2016;327:31–72.

[8] Babikov YL, Mikhailenko SN, Barbe A, Tyuterev VG. S&MPO – An Information System for Ozone Spectroscopy on the WEB. J Quant Spectrosc Radiat Transf 2014;145:169–96. (doi:10.1016/j.jqsrt.2014.04.024)

[9] Birk M, Hausamann D, Wagner G, Johns JW. Determination of line strengths by Fourier-transform spectroscopy. Appl Opt 1996;35:2971–85.

[10] Guelachvili G. Chapter 1 - Distortions in Fourier Spectra and Diagnosis. Spectrometric Techniques Volume 2. Academic press 1981. doi.org/10.1016/B978-0-12-710402-7.50007-1

[11] Hase F. Improved instrumental line shape monitoring for the ground-based, high-resolution FTIR spectrometers of the Network for the Detection of Atmospheric Composition Change. Atmos Meas Tech 2012;5:603–10.

[12] Ngo NH, Lisak D, Tran H, Hartmann JM. An isolated line-shape model to go beyond the Voigt profile in spectroscopic databases and radiative transfer codes. J Quant Spectrosc Radiat Transf 2013;129:89–100.

[13] Li J, Du Y, Peng Z, Ding Y. Measurements of spectroscopic parameters of CO_2 transitions for Voigt, Rautian, Galatry and speed-dependent voigt profiles near 1.43 μm using the WM-DAS method. J Quant Spectrosc Radiat Transf 2019;224:197–205.

[14] Daneshvar L, Földes T, Buldyreva J, VanderAuwera J. Infrared absorption by pure CO_2 near 3340cm^{-1}: Measurements and analysis of collisional coefficients and line-mixing effects at sub atmospheric pressures. J Quant Spectrosc Radiat Transf 2014;149:258–74.

[15] Barnes J, Mauersberger K. Temperature Dependence of the Ozone Absorption Cross Section at the 253.7 nm Mercury Line. J Geophys Res 1987 ;92 :14861.

[16] Mauersberger K, Hanson D, Barnes J, Morton J. Ozone Vapor-Pressure and Absorption Cross-Section Measurements - Introduction of an Ozone Standard. J Geophys Res 1987;92:8480.

[17] Hodges J, Viallon J, Brewer PJ, Drouin BJ, Gorshelev V, Janssen C, et al. Recommendation of a consensus value of the ozone absorption cross-section at 253.65 nm based on literature review. Metrologia 2019;56:034001.

[18] Claveau C, Camy-Peyret C, Valentin A, Flaud JM. Absolute Intensities of the ν_1 and ν_3 Bands of $^{16}O_3$. J Mol Spectrosc 2001;206:115–25. doi:10.1006/jmsp.2000.8280

[19] De Backer-Barilly MR, Barbe A. Absolute Intensities of the 10-μm Bands of $^{16}O_3$. J Mol Spectrosc 2001;205**:**43–53. doi:10.1006/jmsp.2000.8233

[20] Smith MAH, Devi VM, Benner DC, Rinsland CP. Absolute intensities of $^{16}O_3$ line in the 9-11 μm region. J Geophys Res 2001;106(D9):9909–21.

[21] Thomas X, Von Der Heyden P, De Backer-Barilly MR, Bourgeois MT, Barbe A. Infrared absolute intensities of ozone in the 10 and 5 μm spectral range: New investigations. J Quant Spectrosc Radiat Transf 2010;111;1080–88. doi:10.1016/j.jqsrt.2010.02.001

[22] Birk M, Wagner G, Barbe A, De Backer MR, Rotger M. (2018). ESA SEOM-IAS – Measurement and line parameter database O_3 MIR region, Version 1, 2018. Zenodo. http://doi.org/10.5281/zenodo.1492543.

[23] Birk M, Wagner G, Barbe A, De Backer MR, Rotger M, Flaud JM. ESA SEOM-IAS – Measurement and line parameter database O_3 MIR region, Version 2, 2021. Zenodo. http://doi.org/10.5281/zenodo.1492542.

[24] Barbe A and De Backer MR. Measurements of line positions and intensities of ν_1 and ν_3 transitions. Private communication 2019.

[25] Tyuterev VG, Barbe A, Jacquemart D, Janssen C, Mikhailenko SN, Starikova EN. *Ab initio* predictions and laboratory validation for consistent ozone intensities in the MW, 10 and 5 μm ranges. J Chem Phys 2019;150:184303. https://doi.org/10.1063/1.5089134.

[26] Polyansky O, Zobov NF, Mizus II, Kyuberis AA, Lodi L, Tennyson J. Potential energy surface, dipole moment surface and the intensity calculations for the 10 μm, 5 μm and 3 μm bands of ozone. J Quant Spectrosc Radiat Transf 2018;210:127–35. (doi:10.1016/j.jqsrt. 2018.02.018)

[27] Wagner G, Birk M, Schreier F, Flaud J-M. Spectroscopic database for ozone in the fundamental spectral region. J Geophys Res 2002;107(D22):4626–43.

[28] Tyuterev V, Barbe A, Mikhailenko S, Starikova E, Babikov Y. Towards the intensity consistency of the ozone bands in the infrared range: ab initio corrections to the S&MPO database. J Quant Spectrosc Radiat Transf 2021;272:107801.

[29] Tyuterev VG, Kochanov RV, Tashkun SA. Accurate ab initio dipole moment surfaces of ozone: First principle intensity predictions for rotationally resolved spectra in a large range of overtone and combination bands. J Chem Phys 2017;146:064304.

[30] Jacquemart D, Makhnev VY, Zobov NF, Tennyson J, Polyansky OL. Synthesis of ab initio and effective Hamiltonian line lists for ozone. J Quant Spectrosc Radiat Transf 2021;269:107651.

Table 1: Experimental conditions of the recorded spectra.

O_3 spectra	Ozone average pressure in the cell in 10^{-3} atm		T in °K	O_2 average pressure in the cell in 10^{-5} atm	
	5µm InSb-Front	10µm MCT-Back		5µm InSb-Front	10µm MCT-Back
SP1	1.5053	1.5035	297.64	1.49	1.75
SP2	0.8576	0.8561	297.79	3.54	3.76
SP3	0.4242	0.4235	297.76	2.79	2.89
SP4	0.1880	0.1876	298.38	2.82	2.89
SP5	0.7867	0.7852	298.04	3.51	3.73
SP6	1.5372	1.5342	298.68	6.36	2.79

Note: Front and Back are referring to the 20 and 5cm absorption path lengths respectively (see description of the H-shaped cell in Paper I [1]).

Table 2: Column parameters issue from LINEFIT.

From ozone transitions at 10 µm							
		Column parameters					
		SP1	*SP2*	*SP3*	*SP4*	*SP5*	*SP6*
MW1:	ILS-SP*i*	1.021	1.021	1.016	1.015	1.021	1.017
1015-1020 cm^{-1}	**ILS-avg**	**1.019**	**1.019**	**1.020**	**1.026**	**1.022**	**1.018**
MW2:	ILS-SP*i*	1.022	1.021	1.020	1.014	1.023	1.017
1025-1030 cm^{-1}	**ILS-avg**	**1.021**	**1.018**	**1.024**	**1.025**	**1.024**	**1.018**
MW3:	ILS-SP*i*	1.023	1.024	1.022	1.016	1.025	1.019
1045-1050 cm^{-1}	**ILS-avg**	**1.022**	**1.022**	**1.026**	**1.026**	**1.026**	**1.020**
MW4:	ILS-SP*i*	1.023	1.023	1.021	1.015	1.024	1.018
1047.9-1053.8 cm^{-1}	**ILS-avg**	**1.022**	**1.020**	**1.025**	**1.026**	**1.025**	**1.019**
MW5:	ILS-SP*i*	1.025	1.025	1.021	1.015	1.024	1.023
1058.6-1062.7 cm^{-1}	**ILS-avg**	**1.024**	**1.023**	**1.025**	**1.026**	**1.024**	**1.024**
From ozone transitions at 5 µm							
		Column parameters					
		SP1	*SP2*	*SP3*	*SP4*	*SP5*	*SP6*
MW1:	ILS-SP*i*	1.045	1.041	1.042	1.026	1.044	1.043
2092.5-2096.3 cm^{-1}	**ILS-avg**	**1.042**	**1.041**	**1.043**	**1.041**	**1.045**	**1.044**
MW2:	ILS-SP*i*	1.044	1.041	1.041	1.026	1.043	1.043
2096.7-2101.2 cm^{-1}	**ILS-avg**	**1.041**	**1.042**	**1.042**	**1.042**	**1.044**	**1.044**
MW3:	ILS-SP*i*	1.044	1.041	1.042	1.027	1.042	1.042
2116.5-2121.5 cm^{-1}	**ILS-avg**	**1.041**	**1.041**	**1.043**	**1.042**	**1.043**	**1.044**
MW4:	ILS-SP*i*	1.042	1.039	1.040	1.023	1.039	1.040
2121.5-2125.8 cm^{-1}	**ILS-avg**	**1.039**	**1.039**	**1.040**	**1.039**	**1.040**	**1.042**

Note: The lines noted ILS-SP*i* correspond to column parameters obtained for ILS retrieval of spectrum SP*i* whereas the lines noted ILS-avg correspond to column parameters when ILS has been fixed to the averaged LINEFIT-ILS (see text).

Table 3: Average values of intensity ratios issue from Fig. 3 when testing the impact of ILS on MSF (SP1-6) line intensity retrievals. Statistical uncertainties (1σ) after "±" sign are given.

Average ratios	10 μm	5 μm
$\langle S_{ILS-SP1}/S_{This\ work} \rangle$	1.0016±0.0003	1.0026±0.0003
$\langle S_{ILS-SP2}/S_{This\ work} \rangle$	0.9999±0.0004	1.0000±0.0002
$\langle S_{ILS-SP3}/S_{This\ work} \rangle$	0.9955±0.0009	0.9990±0.0004
$\langle S_{ILS-SP4}/S_{This\ work} \rangle$	0.9875±0.0029	0.9833±0.0011
$\langle S_{ILS-SP5}/S_{This\ work} \rangle$	0.9990±0.0004	0.9991±0.0002
$\langle S_{ILS-SP6}/S_{This\ work} \rangle$	0.9990±0.0004	0.9983±0.0002
$\langle S_{R=0.575mm}/S_{This\ work} \rangle$	1.0000±0.0015	1.0079±0.0012
$\langle S_{R=0.545mm}/S_{This\ work} \rangle$	0.9952±0.0015	1.0007±0.0011

Table 4: Comparisons between measurements from this work and from literature. Averaged values of ($\sigma_{this\ work} - \sigma_{Ref}$) and ($S_{this\ work} / S_{Ref}$) are presented with statistical uncertainties (1σ) after "±" sign.

Ref.	Bands	Number of compared transitions	$\langle\sigma_{this\ work} - \sigma_{Ref}\rangle$ in 10^{-5} cm^{-1}	$\langle S_{this\ work} / S_{Ref}\rangle$
		Measurements around 10 µm		
Claveau et al. 2001 [18]	ν_1, ν_3	68	–2±29	1.027±0.019
De Backer et al. 2001 [19]	ν_1, ν_3	106	8±6	1.031±0.018
Smith et al. 2001 [20]	ν_1, ν_3	273	2±3	0.978±0.017
Thomas et al. 2010 [21]	ν_1, ν_3	17	0±3	1.037±0.014
Barbe and De Backer [24]	ν_1, ν_3	222	–10±4	0.997±0.009
Birk et al. 2018 [22]	$\nu_1, \nu_3, \nu_2+\nu_3 - \nu_2$	493	3±2	0.999±0.019
		Measurements around 5 µm		
Thomas et al. 2010 [21]	$\nu_1+\nu_3$	10	3±9	1.038±0.006

Table 5: Statistics of comparisons between measurements from this work and calculations from literature. Average values of ($\sigma_{this\ work} - \sigma_{Ref}$) and ($S_{this\ work} / S_{Ref}$) are presented with the dispersion of the data (1σ) indicated after the "±" sign.

Reference		Number of common transitions*	$\langle\sigma_{this\ work}-\sigma_{Ref}\rangle$ in 10^{-5} cm^{-1}	$\langle S_{this\ work}/S_{Ref}\rangle$
Hamiltonian calculations				
HITRAN 1996 [6]	ν_3	476	8±4	0.987±0.007
	ν_1	18	6±8	0.981±0.011
	$\nu_2+\nu_3-\nu_2$	3	0±11	0.975±0.019
	$\nu_1+\nu_3$	316	6±15	1.003±0.019
	$2\nu_3$	3	0±19	0.961±0.008
HITRAN 2016 [2]	ν_3	476	2±2	1.022±0.006
	ν_1	18	2±5	1.021±0.012
	$\nu_2+\nu_3-\nu_2$	3	0±11	1.014±0.020
	$\nu_1+\nu_3$	316	–3±8	1.042±0.004
	$2\nu_3$	3	3±5	1.035±0.006
GEISA 2015 [7]	ν_3	476	2±2	1.022±0.006
	ν_1	18	2±5	1.021±0.012
	$\nu_2+\nu_3-\nu_2$	3	3±5	1.003±0.017
	$\nu_1+\nu_3$	316	–4±48	1.019±0.008
	$2\nu_3$	3	4±2	1.003±0.010
S&MPO 2019 [8]	ν_3	476	8±2	1.021±0.007
	ν_1	18	7±6	1.020±0.012
	$\nu_2+\nu_3-\nu_2$	3	–13±5	1.010±0.017
	$\nu_1+\nu_3$	316	–3±8	1.042±0.004
	$2\nu_3$	3	3±5	1.035±0.006
S&MPO 2020-d [8]	ν_3	476	4±2	0.997±0.008
	ν_1	18	–2±7	0.999±0.012
	$\nu_2+\nu_3-\nu_2$	3	–13±5	0.995±0.017
	$\nu_1+\nu_3$	316	–3±8	1.000±0.004
	$2\nu_3$	3	3±5	0.993±0.006
URCA_ESA [22,23]	ν_3	476	4±2	0.997±0.008
	ν_1	18	–2±7	0.999±0.013
JMF_ESA [23]	ν_3	475	3±2	0.999±0.006
	ν_1	18	1±4	1.001±0.012
	$\nu_2+\nu_3-\nu_2$	3	2±6	0.993±0.016
Ab-initio calculations				
PES [25] and DMS [25]	ν_3	184	N.A.	0.989±0.005
	$\nu_1+\nu_3$	179		1.005±0.004
PES [26] and DMS [29]	ν_3	476	N.A.	0.988±0.006
	ν_1	18		1.027±0.025
	$\nu_2+\nu_3-\nu_2$	3		0.983±0.016
	$\nu_1+\nu_3$	316		0.989±0.004
	$2\nu_3$	3		0.991±0.013
PES [26] and DMS [26]	ν_3	464	N.A.	1.033±0.006
	ν_1	16		1.074±0.019
	$\nu_2+\nu_3-\nu_2$	3		1.028±0.017
	$\nu_1+\nu_3$	303		1.019±0.004
	$2\nu_3$	3		1.014±0.012

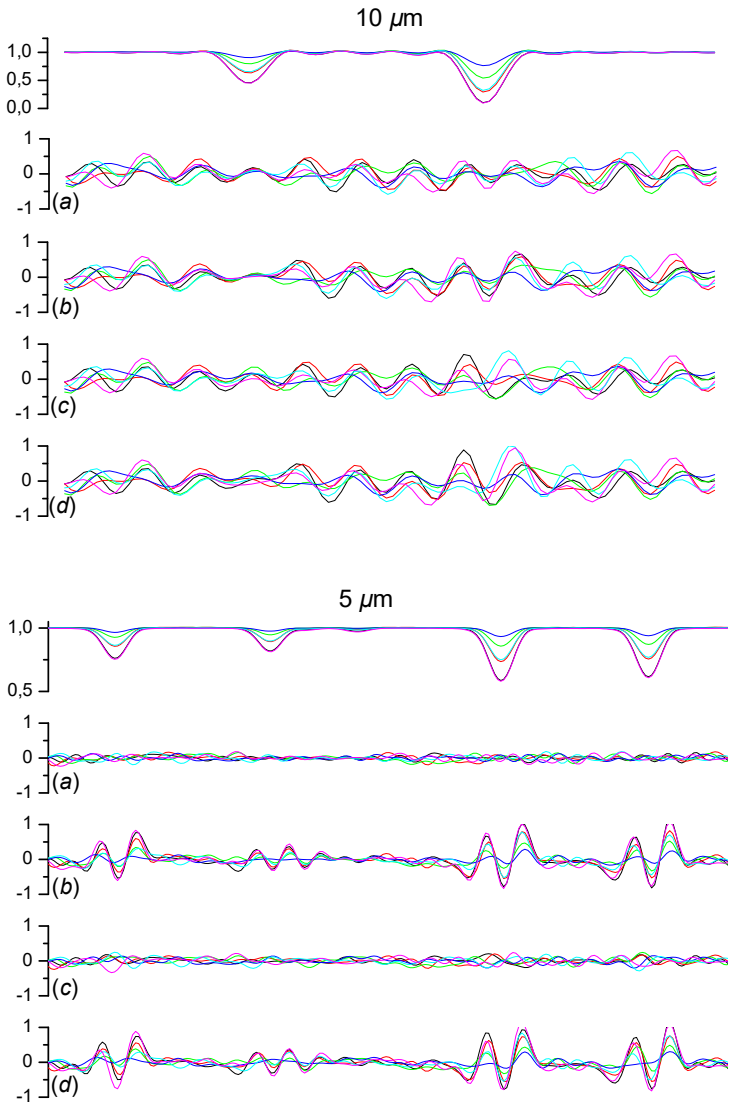

Fig. 1. Experimental spectra (transmittance) recorded at 10 μm and at 5 μm with residuals ((Obs-Calc)/Calc×100 plotted in lower panels) of the fit of ozone transitions between 1054.53 and 1054.58 cm^{-1} (upper figure) and between 2124.07 and 2124.18 cm^{-1} (lower figure). Residuals (*a*) and (*b*) correspond to single spectrum fitting results, whereas residuals (*c*) and (*d*) result from multispectrum fitting. An ideal ILS (R = 0.575 mm) has been used for residuals (*b*) and (*d*), whereas residuals (*a*) and (*c*) are obtained with an average LINEFIT-ILS (averaged ILS derived from spectrum 1, 2, 5 and 6, see text). Identical colors have been employed for all panels: the colors black, red, green, blue, cyan, and magenta correspond to spectra 1 to 6, respectively.

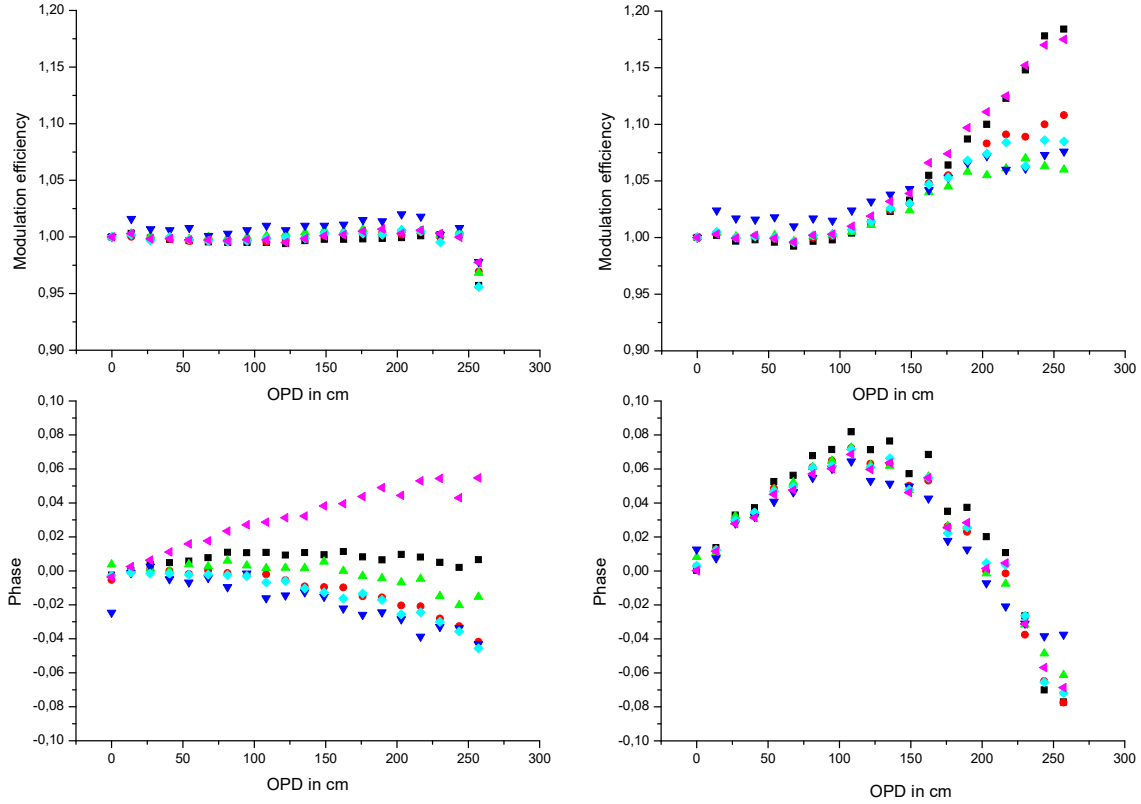

Fig. 2. Modulation efficiency loss and phase (versus optical path depth in cm) retrieved from LINEFIT at 10 μm (left) and 5 μm (right) for the various experimental spectra. The same set of colors as in Fig. 1 has been used to indicate the ILS parameters derived from spectra 1 to 6 (see caption of Fig.1).

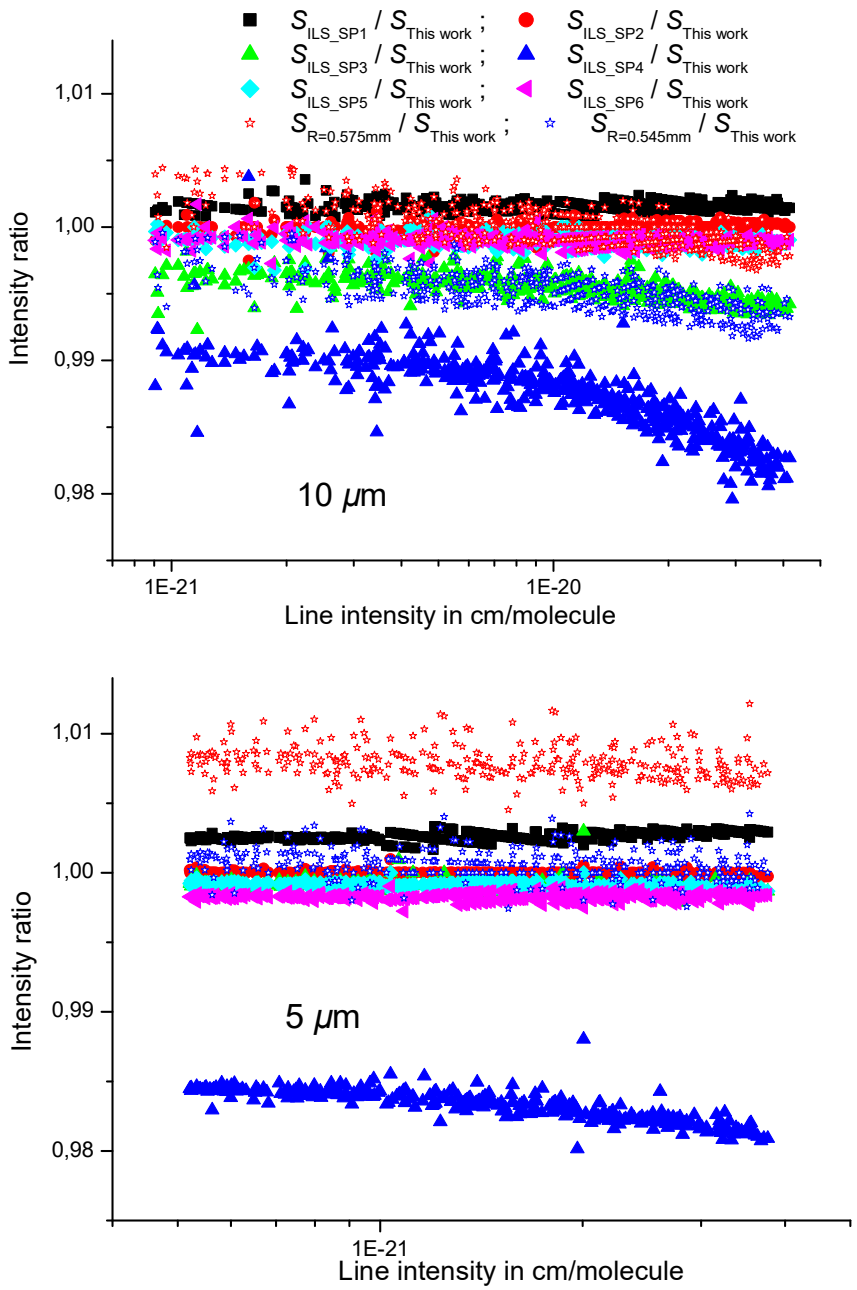

Fig. 3. Intensity ratios for 497 transitions around 10 μm (top) and 319 transitions around 5 μm (bottom) showing the impact of the ILS on line intensities retrieved by multispectrum fitting of spectra 1-6 using a Voigt profile. $S_{\text{This work}}$ corresponds to line intensities using the average of the LINEFIT derived ILSs for spectra 1, 2, 5 and 6. $S_{\text{ILS-SP}i}$ are the line intensities retrieved using the ILS derived from the individual spectrum i (i=1-6) applied to all spectra. $S_{R=0.575\text{mm}}$ and $S_{R=0.545\text{mm}}$ are the intensities retrieved using an ideal ILS calculated with Eqs. (1) and (2) and R = 0.575 mm and 0.545 mm, respectively. The symbols used for intensity ratios are identical at 10 μm and at 5 μm.

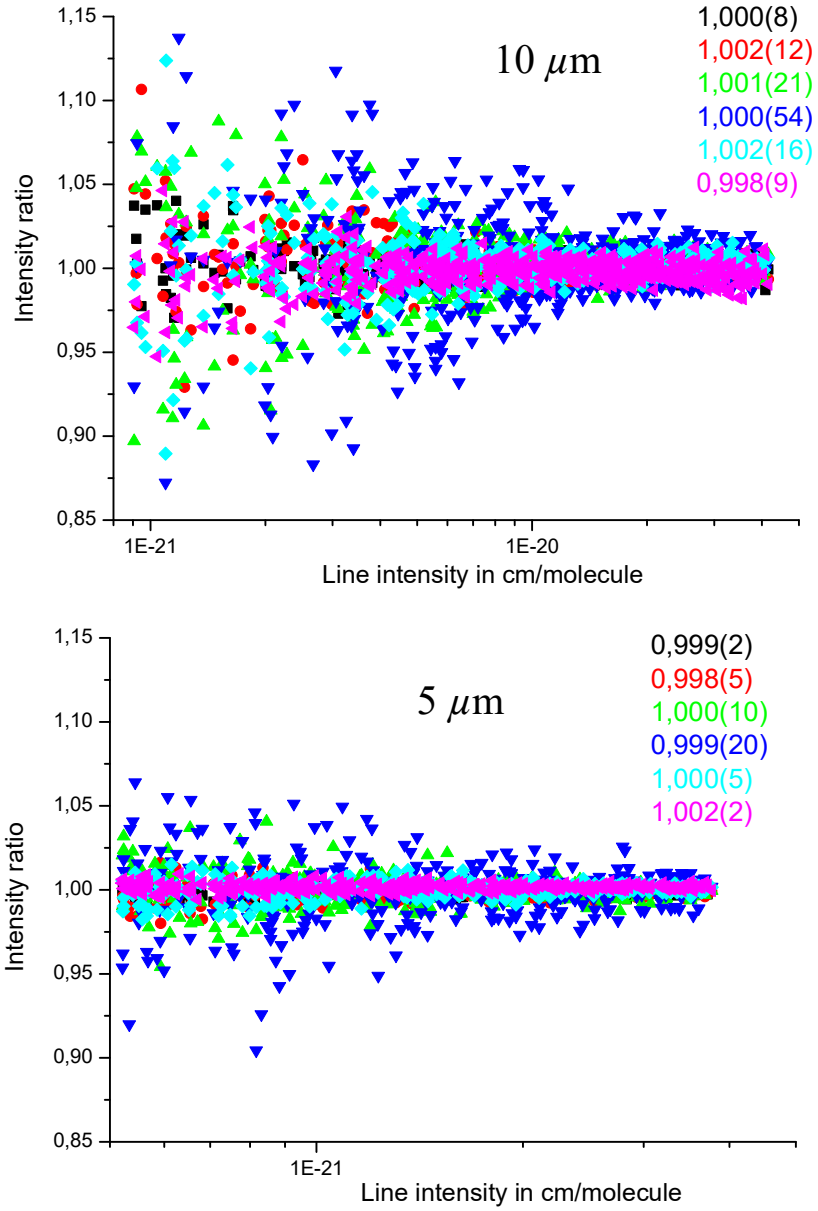

Fig. 4. Dependency of line intensity on spectrum. The averaged LINEFIT-ILS (see text) has been used throughout. Line intensities obtained from single spectrum (i) fitting have been divided by line intensities from multispectrum fitting to all spectra ($S_{\text{this work}}$). Ratios at 10 μm are shown in the upper panel, those at 5 μm are shown at the bottom. Colored symbols indicate the spectrum: black, red, green, blue, cyan, magenta correspond to spectra 1 to 6, respectively. Average values are also displayed and indicated by colors (according to the spectrum number i) and numbers in parentheses designate the statistical uncertainties of the mean (1σ).

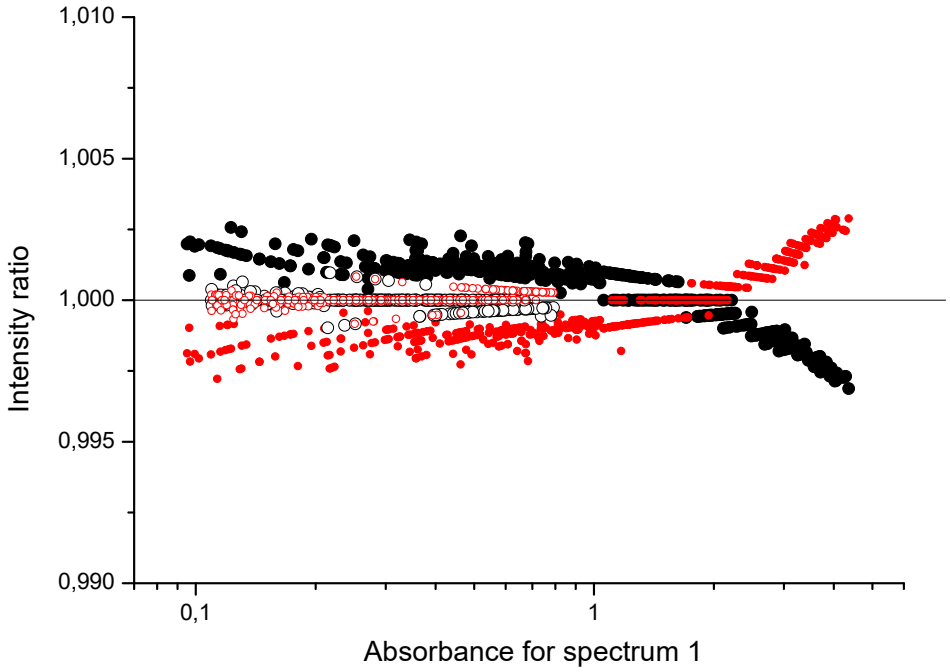

Fig. 5. Sensitivity of line intensities on self-broadening coefficients. The variation of line intensities derived from the multispectrum fitting (with a Voigt profile and the averaged LINEFIT ILS) are shown when the self-broadening coefficients are modified by +5% (black symbols) or -5% (red symbols) as compared to the reference values (HITRAN 2016). Intensity ratios at 10 μm are indicated by solid symbols and those at 5 μm by open symbols.

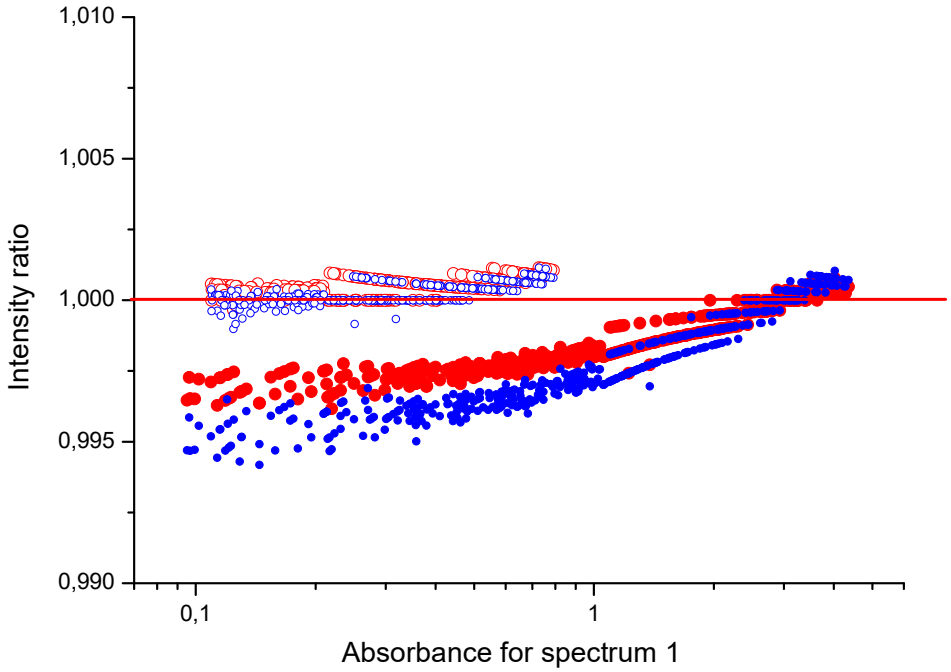

Fig. 6. Molecular line profile dependence of line intensities. Ratio of line intensities (S_{qSDVP} /S_{Voigt}) derived from the qSDVP compared to the Voigt profile is shown both at 10 μm (solid symbols) and at 5 μm (open symbols) as a function of the absorbance under experimental conditions of spectrum 1. Except for the molecular line profile, the same procedure involving the multispectrum fitting of all spectra and obtaining the ILS from LINEFIT using all spectra except 3 and 4 has been applied. Self-broadening coefficients (γ_0) are fixed to those from HITRAN 2016 and quadratic parameters for the qSDVP are set to $\gamma_2 = 0.1\times\gamma_0$ (red symbols) or $\gamma_2 = 0.15\times\gamma_0$ (blue symbols). See text for more details.

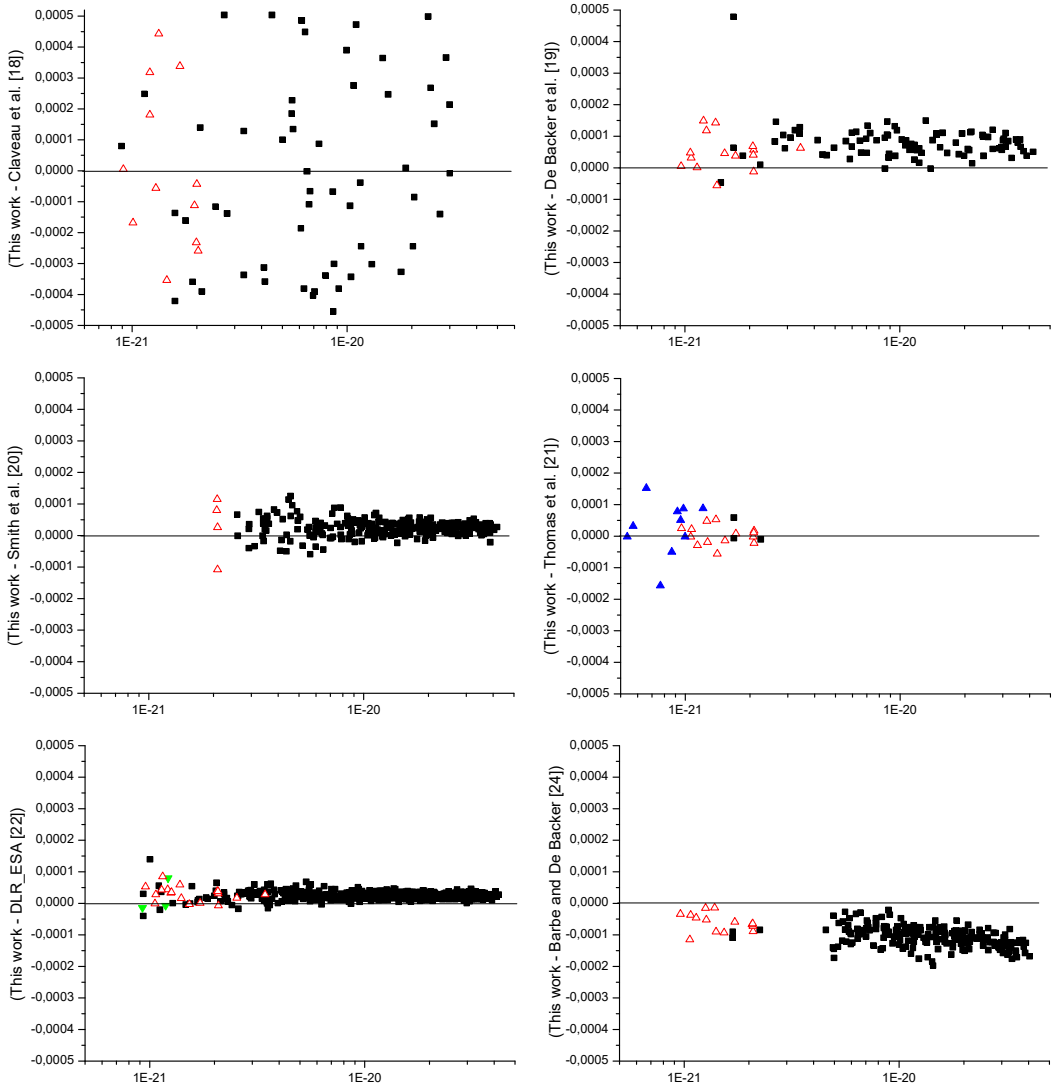

Fig. 7. Comparison of experimentally derived line positions at 5 μm and 10 μm. The difference of line positions (in cm^{-1}) is plotted (vertical scale) as a function of the line intensity (in cm/molecule) given on a logarithmic scale. The same scale has been used for all panels to facilitate comparisons between measurements from literature. The reference for each panel is indicated on the ordinate axis. Solid black squares correspond to measurements of ν_3 transitions, red open triangles designate ν_1 transitions and solid green downside triangles indicate the $\nu_2+\nu_3-\nu_2$ band at 10 μm. $\nu_1+\nu_3$ transitions in the 5 μm range are indicated by solid blue triangles.

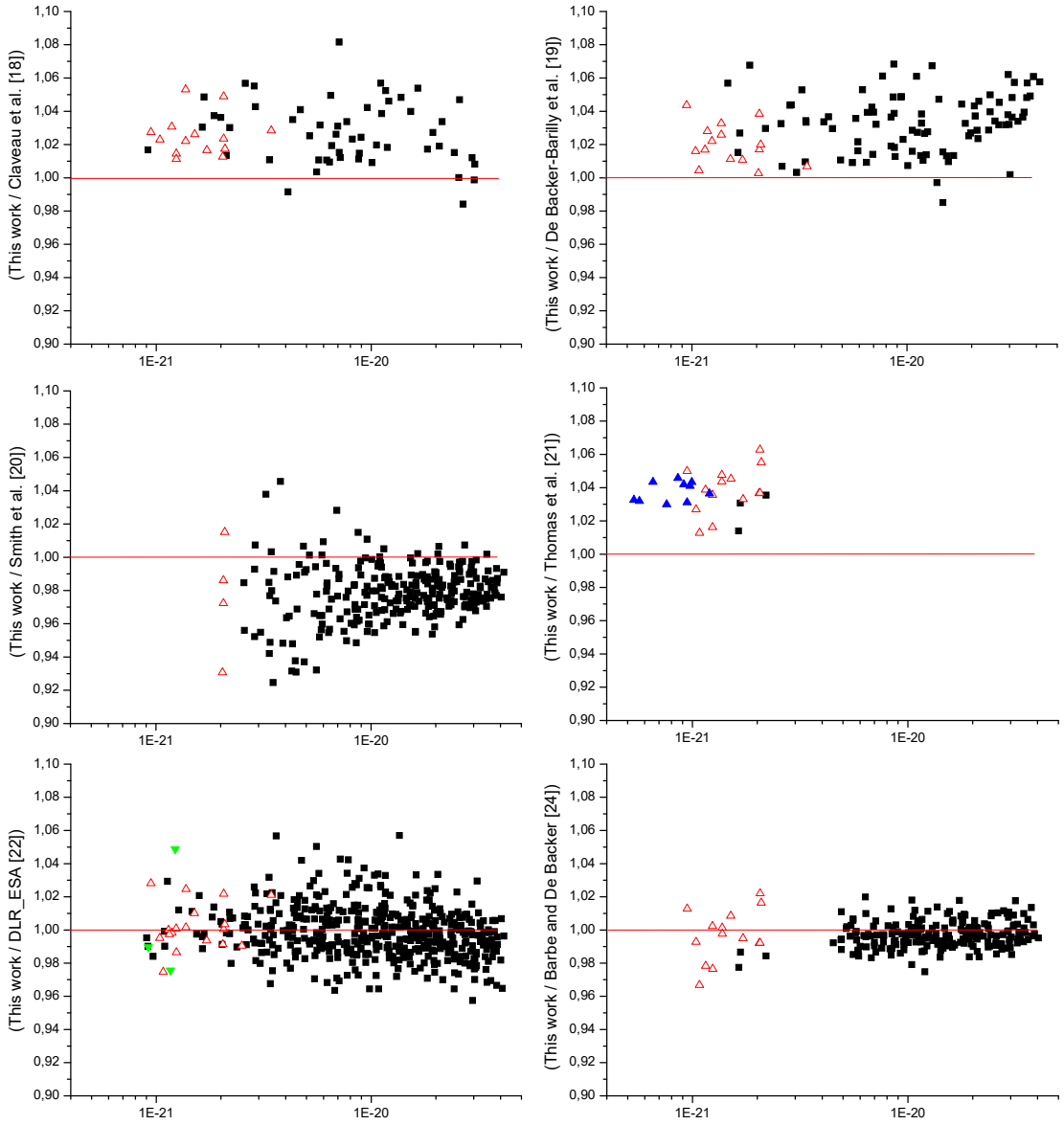

Fig. 8. Comparisons between experimental line intensities at 5 μm and 10 μm (see Fig. 7 for symbols and references). Ratios between our measurements and experimental data from the literature are plotted as a function of line intensity (in cm/molecule), given on a logarithmic scale. All panels are given on the same scale to facilitate comparisons.

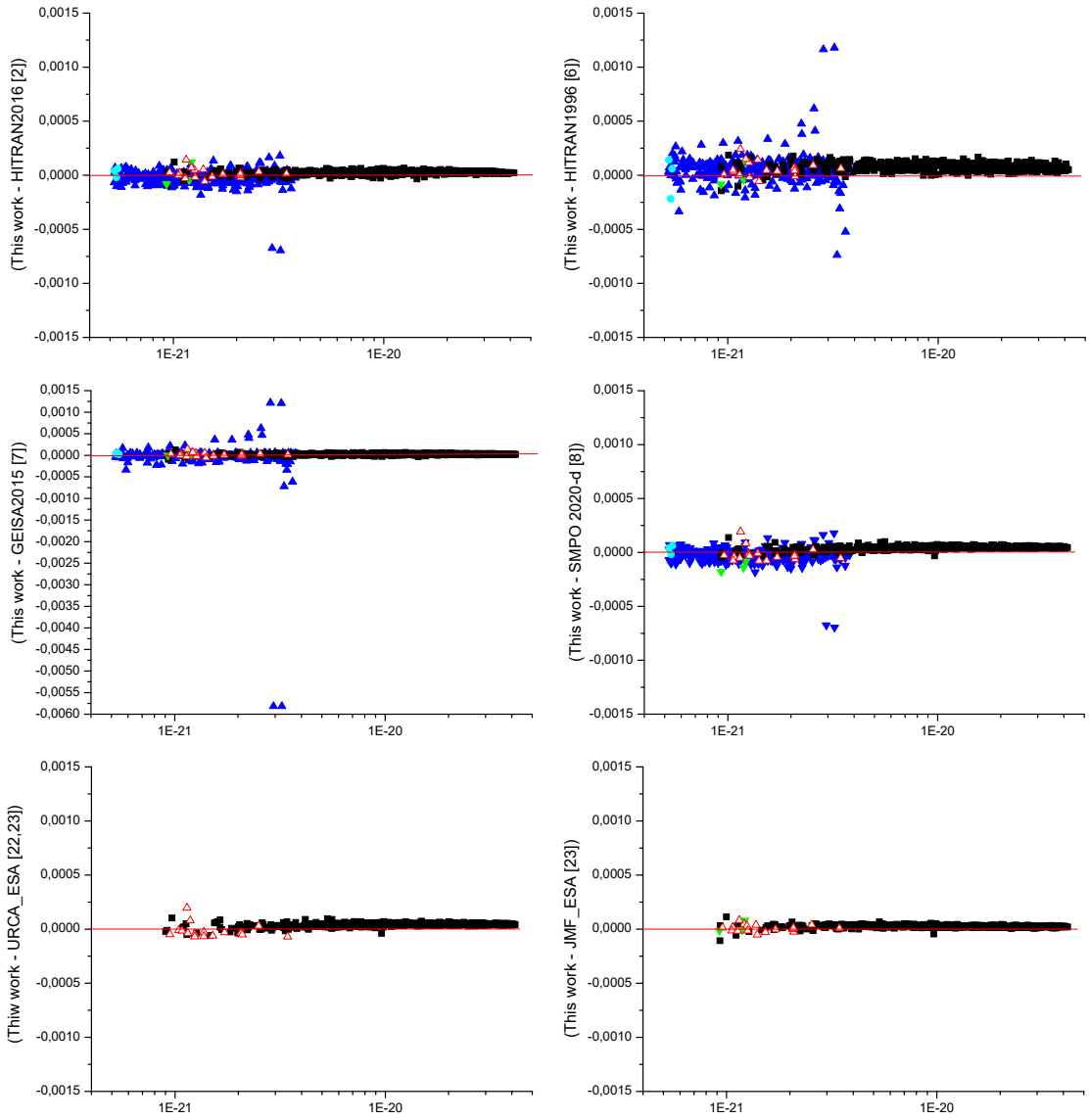

Fig. 9. Comparison with calculated line positions at 5 μm and 10 μm. Experimentally determined line positions of this work are compared to calculations and databases values. The difference of line positions is plotted in cm^{-1} (vertical scale) as a function of the line intensity in cm/molecule, given on a logarithmic scale. Solid black squares correspond to the ν_3 band, red open triangles are used for the ν_1 band and solid downside triangles for the $\nu_2+\nu_3-\nu_2$ band at 10 μm. $\nu_1+\nu_3$ transitions in the 5 μm range are indicated by solid blue triangles whereas solid cyan circles correspond to transitions in the $2\nu_3$ band.

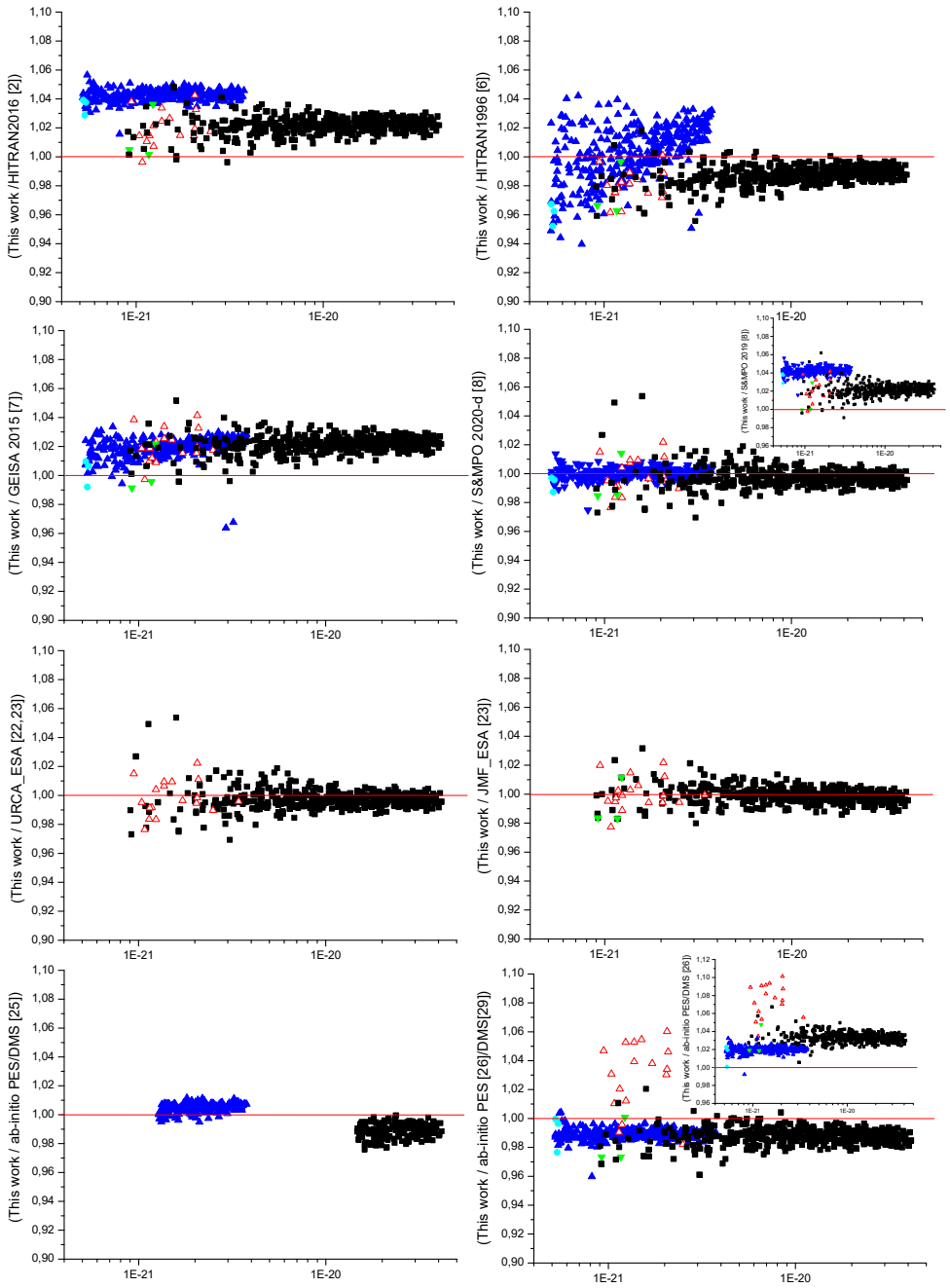

Fig.10. Comparison with calculated line intensities at 5 μm and 10 μm (see Fig. 9 for symbols). Ratios between our measurements and calculated data from the literature or databases ($S_{\text{This work}}$ / $S_{\text{Reference}}$) are plotted as a function of line intensity in cm/molecule, given on a logarithmic scale.